Effect of material properties in CFRD Tailing–Embankment Bridge During a Strong Earthquake

Article · January 2013

Behrouz Gordan
Islamic Azad University, Gorgan, Iran

Caspian Journal of Applied Sciences Research
2(11), pp. 61-72, 2013
Journal Homepage: www.cjasr.com
ISSN: 2251-9114

Effect of material properties in CFRD Tailing-Embankment Bridge During a Strong Earthquake

Behrouz Gordan [1], Azlan Bin Adnan [2,*]

[1] *Department of Geotechnic &Transportation Faculty of civil Engineering, University Teknologi Malaysia 81310 Skudai, Johor, Malaysia*

[2] *Earthquake Department, University Technology Malaysia 81310 Skudai, Johor, Malaysia*

Bridge design is very costly when valley is very long. In this situation, bridge length can be reduced by use of two tailing embankments. In terms of literature, structural performance and interaction between dam with abutment or bridge showed significant role during an earthquake on dynamical assessment. The seismic behavior is affected by modulus ratio between transmission zone and concrete slab. This paper tried to evaluate the effect of physical properties based on different conditions of concrete slab and cushion zones to attain the optimum ratio in order to strong earthquake effect. The numerical result was collected at the end of construction based on half height of tank. ANSYS 13 program was used by Finite-Element method. As results, the optimum comportment was obtained when compressive strength of concrete slab was 45 mega pascal and modulus elasticity ratio (between cushion and embankment body) was equal eight. Consequently, an expanding joint is required between tailing embankment and bridge to avoid of impact force.

Keywords: CFRD; Cushion; Concrete slab; Numerical analysis; Earthquake

1. Introduction

One of the most significant current discussions in civil engineering is a dynamic analysis of an earth dam. This process was started after some major damages in dam during the earthquake. There is some tremendous damage that failure mechanism was occurred after cracks making in the dam body. Besides, some phenomena before than failure phase like piping or overflow were previously experienced. However, this analysis was concluded with respect to specific carefulness to avoid of the structural failures in high level of seismic zone. Furthermore, the construction technique is a step by step with respect to compaction procedure in embankment. Hence, the static settlement can be closed by consolidation process. After that, the dynamical settlement can be driven by structural excitation under the seismic loading. In addition, data monitoring based on literature indicated that, there is a little bit information in this domain (Zeghal et al, 1992 and Gikas et al, 2008). Furthermore, Concrete Face Rock-fill Dam (CFRD) engineering is recently dedicated maturity situation in many aspects. They are covered by some factors like foundation design, building materials, criteria, and compaction method with procedure zoning. However, it was particularly depended on opinion of experience and engineering (Cooke, 1984- Cooke et al, 1987 and Núñez, 2007). In terms of the construction in the high seismic zone, structural behavior can be significantly affected by strong earthquake. Therefore, security feature is located at the main concern of design procedures. The plastic deformation and settlement without change of slope in its classical sense were featured by CFRD structure (Gazetas et al, 1992; Makdisi et al, 1978;

* Corresponding address: Earthquake Department University Technology Malaysia 81310 Skudai, Johor, Malaysia
E-mail address: azelan_fka_utm@yahoo.com (Mohsen Rajabi)

Newmark, 1965 and Seed, 1979). In terms of design, concrete face consisted of an earthquake loading poses additional challenges while the physical face is just a water stop only. Besides, it is structural element of the dam's configuration. Therefore, the behavior must be seriously checked at the design stage. To date, the design effort has been limited to avoid of failure and included minimize cracking. It can be ensured valid behavior of concrete joints. Moreover, materials have chosen to avoid of the generate pore pressures to develop in the dam's body during and after strong seismic loading (Sherard et al, 1987). Some methods were used (Makdisi et al, 1978; Newmark, 1965 and Sherard et al, 1987) to evaluate earthquake-induced dam deformation range from simple analytical tools regard to three dimensional (3D) numerical models. In recent years, numeric analysis to evaluate structural behavior (CFRD) during dynamic loading was carried out (Kong et al 2010 and Bayraktar et al 2011). Not only, lack of information in terms of data monitoring but also development technology caused to use numerical analysis. These programs are performed based on both techniques like Finite-Element Method (FEM) or Finite-Difference Method (FDM). In brief, well-designed and properly compacted on rock foundations is shown safe under strongest earthquake (Wieland et al, 2007). Though, the structural behavior is not completely clear in this domain with respect to litrature. The stress control in slab was noted by major goal to avoid of cracks and joints in the slab. This paper tried to evaluate an effect of modulus elasticity in the slab, and transmission zone under the seismic vibration by planE strain method (2D) using ANSYS program.

2. Modeling Process

In terms of numerical analysis, the modeling procedure is explained step by step below.

2.1. Introduce ANSYS software and elements

This program is very comprehensive based on Finite-Element Method (FEM) with 100000 code line, as It's related to computer-aided engineering (CAE) . In fact, it's famous in most of Finite-Element software. In this paper, Solid42 element for dam body with foundation, and Fluid79 element for water reservoir are respectively applied with respect to (2D) condition. However, both are recommendation by ANSYS Help menu.

2.2. Boundary conditions

The boundary condition is focused on three lines. One of them has located at bedrock. Other lines are placed at parallel situation with perpendicular status at both sides of model. In order to one dimensional vibration, bedrock is trembled by NAGAN earthquake at horizontal direction. In terms of program ability in ANSYS 13, input data was used based on displacement-time instead of acceleration-time. Because distribution of displacement at the crest which connected by bridge was the main purpose. Therefore, this record is converted to displacement-time by SISMOSOFT3 software. Also, horizontal earthquake for dynamical assessment were used by most of the researchers based on literature, because more probability it's occurred in compare vertical vibration. Moreover, in terms of slope stability, dam is safe under vertical earthquake. In fact, safety factor for horizontal earthquake can be dramatically reduced. Finally, horizontal earthquake was used. This earthquake involved sub steps of time equal to 0.02 seconds. In addition, vertical and horizontal displacement are respectively used same zero and 0.01 meters in parallel lines. However, the transient characteristic of solid material can be occurred by horizon displacement. It is a main assumption in terms of elasticity equilibrium during seismic waves. In fact, vertical displacement in both line at right and left side of foundation are zero with respect to the static condition. Also, horizontal displacement in both lines as mentioned are 0.01 meter with respect to possibility of wave transmission during vibration, because model did not run while it was at zero. In order to result accurate, this value is exactly obtained based on trial and error method.

2.3. Model parameters

Figure 1 shows model parameters with different zone in embankment. The model dimension is shown in Table 1.

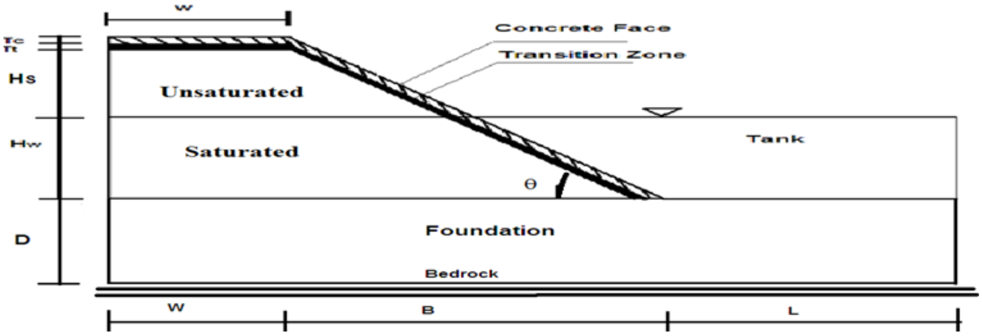

Figure 1: Parametric Dimension of models

Table 1: Models dimension

w	B	L	D	Hw	Hs	Tt	Ts	θ
20.00m	30.00m	15.00m	10.00m	10.00m	9.40m	0.30m	0.30m	33.42

Table 2: Material Properties

Zone	Material	Density (Kg/m^3)	Elasticity Modulus (Kg/m^2)	Poisson Ratio	Yield stress (Kg/m^2)	Tangent Modulus (Kg/m^2)	Coefficient Friction
1	Water	1000	1E15	0.49	---------	-------	0.001
2	Saturated soil	900	1E6	0.30	2000	2020	0.20
3	Unsaturated soil	1900	1.50E6	0.45	3000	3030	0.20
4	Transmission1-loose sand saturate	800	5E6	0.30	10000	10100	0.10
5	Transmission1-loose sand Unsaturated	1800	8E6	0.30	16000	16160	0.10
6	Transmission2-Moderate Sand saturated	800	10E6	0.30	20000	20200	0.10
7	Transmission2-Moderate sand Unsaturated	1800	16E6	0.30	32000	32320	0.10
8	Concrete slab-1	2400	2.12E9	0.20	----------	----------	0.30
9	Concrete slab-2	2400	2.60E9	0.20	----------	----------	0.30
10	Concrete slab-3	2400	3.00E9	0.20	----------	----------	0.30
11	Foundation- Sand saturated	800	2.00E6	0.30	4000	4040	0.10

2.4. Material properties & introduce of model

This part introduced five section properties such as water, foundation, embankment body, transmission zone and concrete slab. They are consisted of both situations like saturated or unsaturated. Table 2 described all materials for non-linear modeling according to the bilinear method with hardening-softening technique. However, tangent modulus was a gradient of second line based on simulation of soil behavior. In fact, soil was modeled by two lines. The first line shows elastic zone based on modulus elasticity. The second line shows elastic-plastic and plastic zone and defined by tangent modulus. The unit measurement of tangent modulus was same modulus elasticity and yeild stress with kilogram over square meter. Finally, the value of tangent modulus was mostly 0.01 in order to slope in sand based on literature. In addition, the foundation material was loose sand in order to river condition. The unit measurement of density was kilograms over cube meter when it was meter for model length. Moreover, three concrete slab face and two transmission zone in order to different modulus elasticity were applied. Besides, water modulus and coefficient of Poisson's ratio equal to 1E15 (kilograms over square meter) and 0.49 were respectively applied. Both have recommended to satisfy the incompressible condition of fluid water by LIQUID ANSYS. In parallel, the coefficient friction was used for interface between different materials. Finally, material properties have been referenced (Mestat Ph, 1993).

Model name and material properties in each model is shown in Table 3.

Table 3: Introduce of Models

Model name	Tank	Non- Saturated State	Saturate State	Foundation	Concrete slab	Transmission Zone
Initial (CS1-T1)	1	2	3	11	8	4&5
Secondary (CS2-T1)	1	2	3	11	9	4&5
Third (CS3-T1)	1	2	3	11	10	4&5
Forth (CS1-T2)	1	2	3	11	8	6&7

In terms of concrete slab, material properties for different situation are shown in Table 4.

Table 4: Concrete Slab Properties

Zone	Density (Kg/m^3)	Elasticity Modulus (Kg/m^2)	Poisson's Ratio	Strength after 28 days curing (MPA)
Concrete slab-1 (CS1)	2400	2.12E9	0.20	38.00
Concrete slab-2 (CS2)	2400	2.60E9	0.20	42.00
Concrete slab-3 (CS3)	2400	3.00E9	0.20	45.00

2.5. Key points and meshing

Figure 2 shows regular mesh with respect to optimum effect of interaction. It is carried out by node to node method in models. Moreover, Figure 3 shows fourteen main points in each model in order to compare analysis.

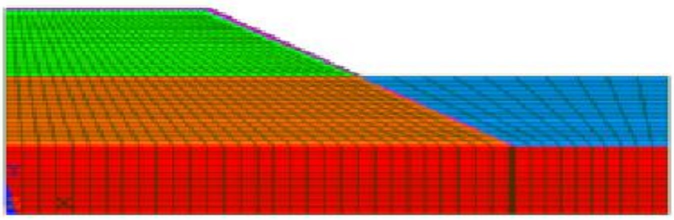

Figure 2: Mesh of the initial model with regular method

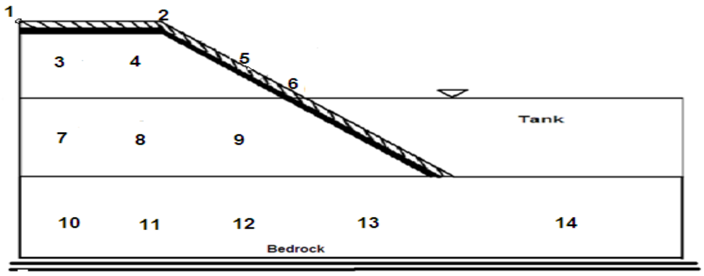

Figure 3: Key points of models

2.6. Earthquake recording

All models in this research are simulated by NAGAN record. This record included acceleration-time with 5.02 seconds in order to duration, also peak ground acceleration (PGA) was 0. 65g. Figure 4.a shows acceleration time. This record based on seismosoft 3 program is respectively converted to velocity time and cumulative displacement time, as can be seen in Figure 4.b and Figure 4.c.

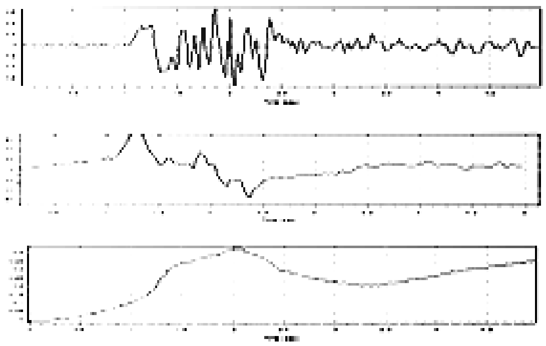

Figure 4: Convert acceleration-time by SEISMOSOFT3 Software

After that, the cumulative displacement is converted to displacement-time by Excel program. Figure 5 shows displacement-time for input data. However, the main purpose of this research was evaluate of displacement distribution at the crest during earthquake in order to compute space between embankment and bridge. Therefore, time – displacement is used.

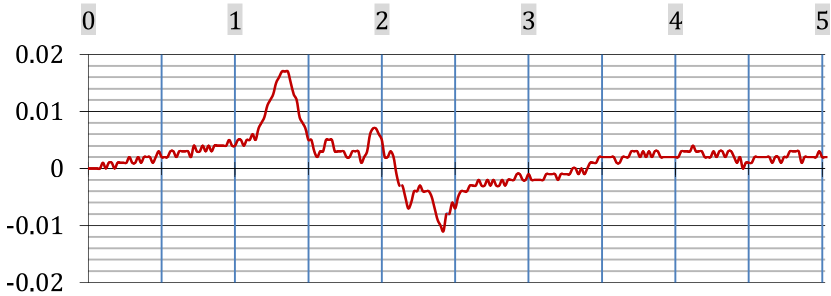

Figure 5: Input data of NAGAN earthquake record (Displacement-Vertical axis (meter) and time-horizontal axis (second)).

This Figure indicated that, maximum and minimum displacements are respectively located at 16.5 mm, and 11 mm.

3. Results & Analysis

Numerical analysis is carried out for all models. Distribution of some factors in main points like displacement, shear strain and shear stress will be discussed. Figure 6 and Figure 7 show distribution of horizontal displacement in different models. The vertical axis shows displacement with meter unit measurement. It is worth noting that, maximum absolute displacement is located at the crest, as can be seen in Figure 6.

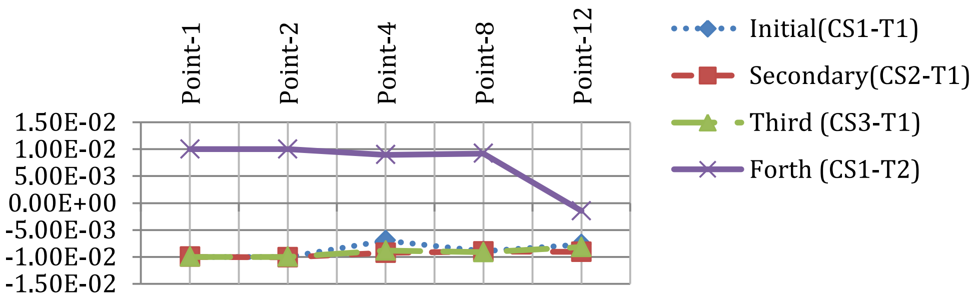

Figure 6: Horizontal displacement in Models1-4. The Vertical axis is the value of horizontal displacement (meter)

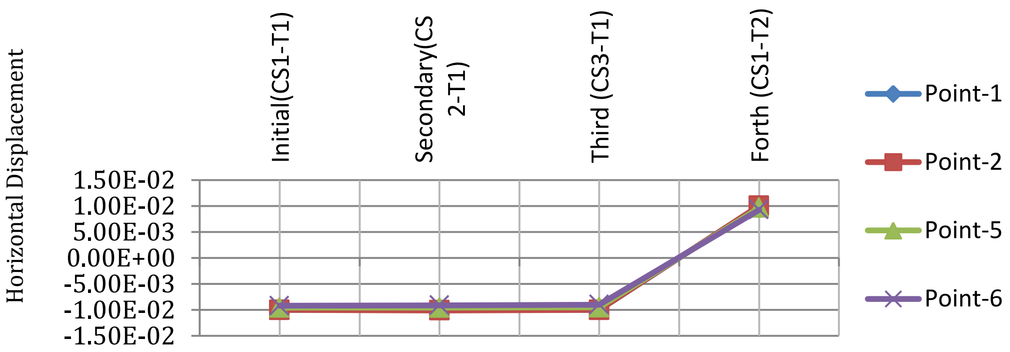

Figure 7: Horizontal displacement at the crest and upstream slab. The vertical axis is horizontal displacement (meter)

It was found that, the space joint is undoubtedly required at the crest. This space was between embankment and bridge. Moreover, the crest zone can be separated by fourth model. This attitude for other models with respect to shrinkage behavior was reversed, as can be seen in Figure 7. Therefore, one of the specific feature during the earthquake like buckling is obtained by fourth model.

Figure 8: Damages of concrete slab Zipingpu dam after Wenchuan earthquake in China

Figure 9: Buckling of canal lining elements In the 21 September 1999 Chi-Chi earthquake in Taiwan

In this context, Figure 8 shows crack after earthquake in concrete slab face of the Zipingpu dam. However, total deformation is function of both displacements like horizontal and vertical. Moreover, Figure 9 shows damage at concrete slab with respect to buckling. Based on both cases as mentioned previously, more research on CFRD structure under seismic loading for control, and reduce damages is very important. In addition, distribution of vertical displacement discussed in Figures 10 to 14. Respectively, horizontal and vertical directions show model name and displacement with meter unit measurement in the end of earthquake.

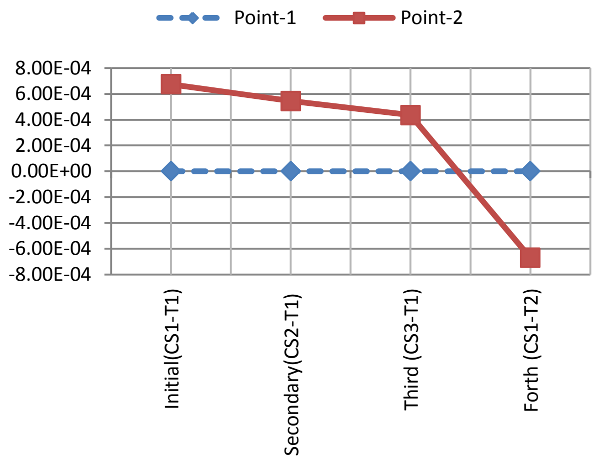

Figure 10: Vertical displacement in Points (1-2). The vertical axis is the value of vertical displacement (m).

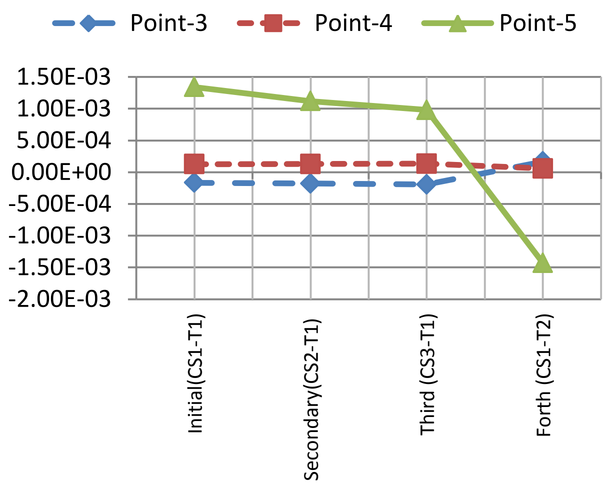

Figure 11: Vertical displacement in Points (3, 4, 5). The vertical axis is the value of vertical displacement (m)

Figure 10 shows distribution of vertical displacements at the both edges of the crest. Relative displacement was located at the best situation in the third model. It is worth noting that, the minimum of absolute value is significant point in order to avoid of cracks making. Also, maximum absolute relative displacement is occurred at initial model and fourth model. On the other hand, fourth model shows negative relative displacement that corresponded to settlement while other models were at uplift situation with respect to positive value. Both models indicated that the damage can generate cracks at the crest. Furthermore, Figure 11 illustrated the third model is the best aspect of the vertical displacement to reduce the possibility of the crack process in the unsaturated zone of embankment.

Figure 12: Tension cracks on Cogoti Dam crest associated earthquake in 1997

Figure 12 illustrated the longitudinal cracks along the crest. It can be seen cracks after earthquake with respect to relative vertical displacement. Figure 13 and 14 show vertical displacement in the upstream and saturated zone, respectively. In terms of absolute displacement, behavior was same at concrete surface. In addition, third model is represented the best situation to satisfy relative displacement and avoid of cracks making in the saturated zone.

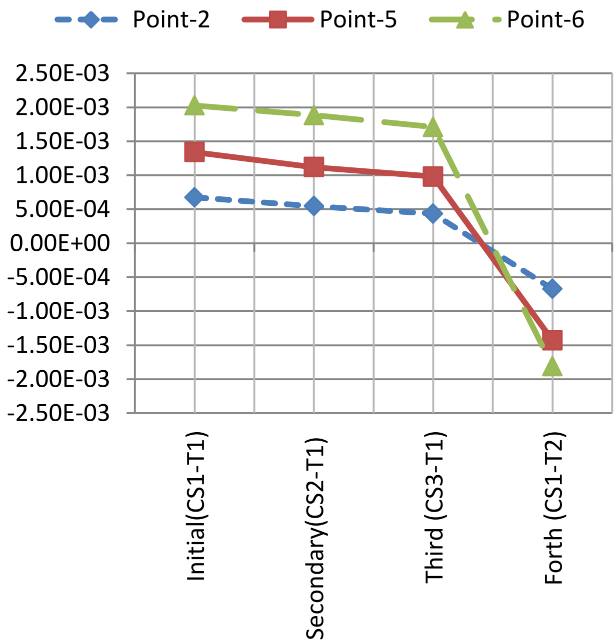

Figure 13: Vertical displacement in the Upstream. The vertical axis is the value of vertical displacement (m).

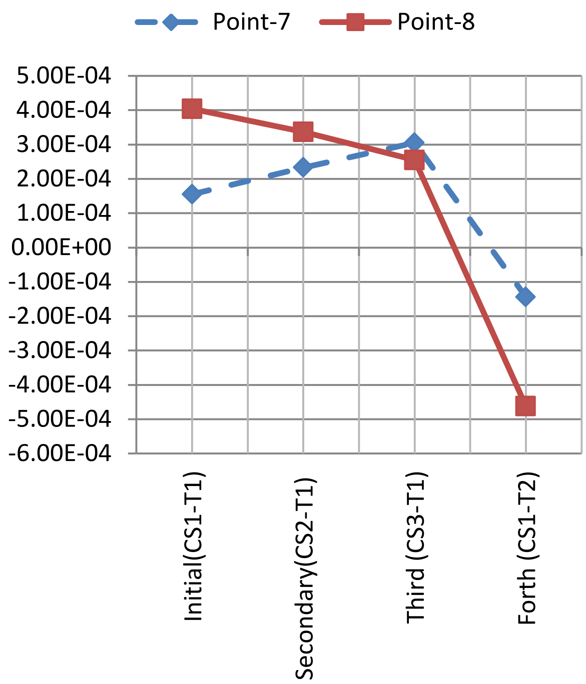

Figure 14: Vertical displacement in Points 7-8. The vertical axis is the value of vertical displacement (m).

As a result, the third model was optimum status in order to minimize relative displacement, and damage was reduced. Besides, distribution of shear stress is significantly compared in models. Figure 15, 16 and 17 show shear stress in different models. The horizontal axis indicated model name, and vertical direction was shear stress based on (kilogram over square meter). In this context, shear stress in some models was negative at the end of dynamic loading. However, main character of the wave transfer in structure observed with respect to change position in sub steps of vibration duration.

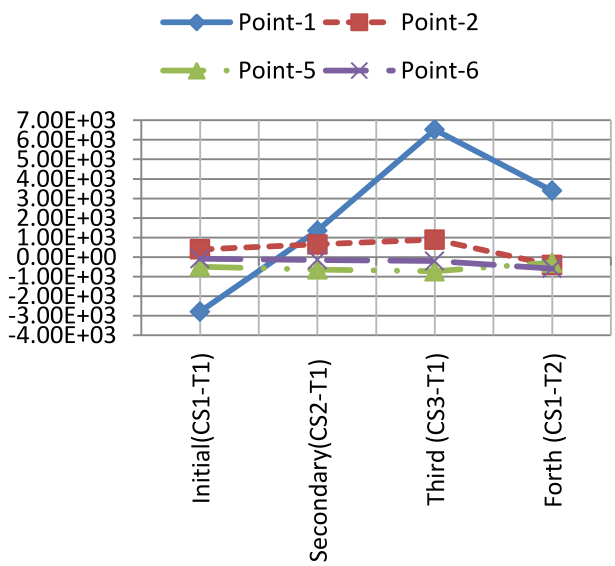

Figure 15: Shear stress XY at the crest and Upstream. Vertical direction is a value of shear stress (kg/m^2).

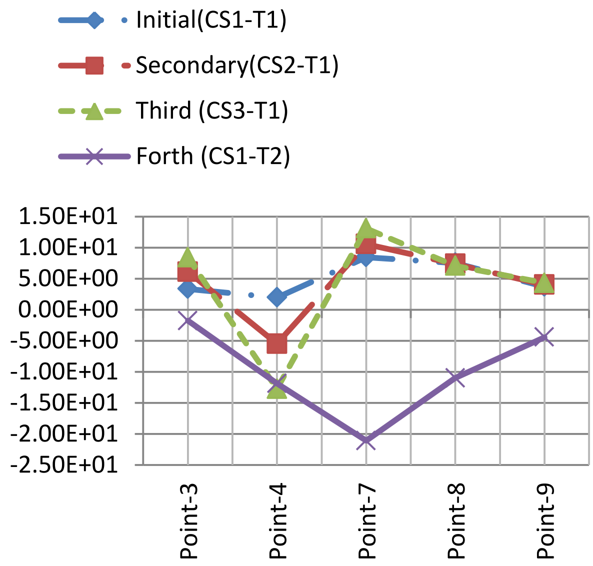

Figure 16: Shear stress XY in saturate and non saturate zones. Vertical direction is a value of shear stress (kg/m^2).

Shear stress distribution in models were compared. Figure 15 shows results at crest and concrete slab face. It was found that, the best situation was obtained by fourth model in order to convergence distribution but this model was eliminated with respect to displacement condition. Consequently, maximum shear stress in concrete slab face at point 1 in third model was obtained. Figure 16 shows shear stress distribution in body embankment, as can be seen convergence results in all points apart from the point 4. However, maximum shear stress was located in third model at point 4. Figure 17 shows shear stress distribution in foundation. In terms of model at second third and fourth situation, convergence results in point 10, point 12 and point 14 were obtained. However, maximum and minimum shear stress was respectively located at point 12 and point 14. After all as discussed, a good behavior during earthquake with respect to displacements and shear stress was obviously appeared by third model.

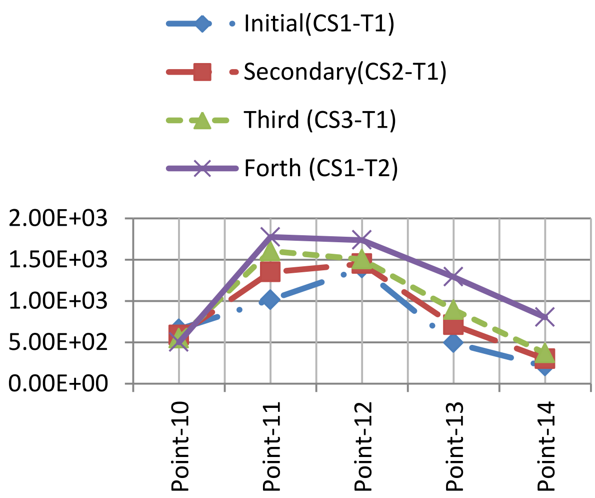

Figure 17: Shear stress XY in the foundation.

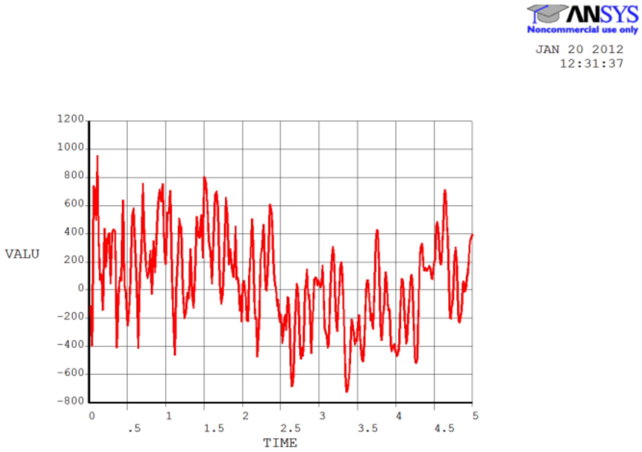

Figure 18: XY Shear stress in the secondary model at point 2.

Besides, Figure 18 and Figure 19 show respectively distribution of shear stress and vertical displacement in each sub step of the earthquake duration. It can be seen that, both factors are changed along time.

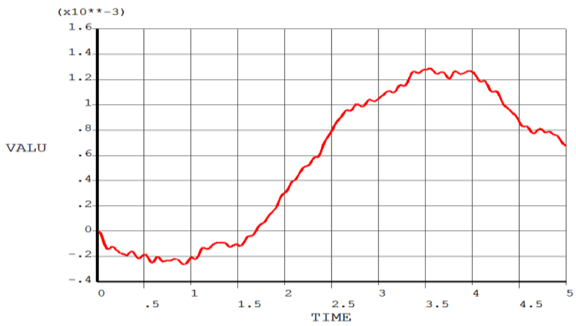

Figure 19: vertical displacement in the secondary model at point 2.

In fact, main character of dynamical aspect in order to transfer waves from bedrock to structure was appeared by soil amplification process. It was very expressive in terms of maximum displacement at the crest. Besides, shear stress changed with negative or positive position at point 2, for instance. Finally, third model referred to satisfy all conditions like both direction deformation and shear stress showed the best behavior during the strong earthquake. The effect of angular abutment on this condition is recommended for next research.

4. Conclusion

The short embankment bridge with CFRD technique was vibrated by strong earthquake (PGA= 0.65g). Different physical properties of the concrete slab and transmission zone were investigated. Displacements in both direction and shear stress are analyzed by plane strain method (2D) in some key points. As results, the optimum comportment was obtained when compressive strength of concrete slab was 45 mega pascal and modulus elasticity ratio (between cushion and embankment body) was equal eight. The expansion joint between bridge and embankment was 1.65 cm required to avoid of impact pressure force. Consequently, this space is recomended 2.00 cm with respect to executive perspectives.

5. Acknowledgements

This study is made possible by the support of the International Doctorate Fellowship of Universiti Teknologi Malaysia, and it is very much appreciated.

References

Bayraktar. A, Emre. M and Adanur. S. (2011). The effect of concrete slab–Rock fill interface behavior on the earthquake performance of a CFR dam. International Journal of Non-Linear Mechanics 46 (2011) 35–46 journal homepage: www.elsevier.com/locate/nlm

Cooke. J. (1984). Progress in rockfill dams. ASCE JGE, 110(10), 1381-1414.

Cooke. J. and Sherard. J. (1987). Concrete-face rockfill dam: II. Design. ASCE JGE, 113(10), 1113-1132.

Gazetas. G. and Dakoulas. P. (1992). Seismic analysis and design of rockfill dams: State of the art. Soil Dynamic Earthquake Engineering, 11(1), 27-61.

Gikas. V and Sakellariou. M. L. (2008). Settlement analysis of the MORNOS earth dam (Greece): Evidence from numerical model and geodetic monitoring. Journal homepage: www.elsevier.com/locate/engstruct Engineering Structures 30 (2008) 3074–3081

Kong. X .J, Y. ZhouY, Xu B , Zou D.G(2010). Analysis on Seismic Failure Mechanism of Zipingpu Dam and Several Reflections of Aseismic Design for High Rock-fill Dam. Earth and Space 2010: Engineering, Science, Construction, and Operations in Challenging Environments © 2010 ASCE http://www.ascelibrary.org

Makdisi F. and Seed B. (1978). Simplified procedure for estimating dam and embankment earthquakes induced deformation. ASCE JGE, 104(7), 849-867.

Mestat, ph. (1993). “Lois des Comportement des Geomateriaux et Modelisation Par La Methode Des “Elements finis”, Etudes et Recherches des Laboratories des Ponts et Chaussees- Serie Geotechnique: GT52

Newmark. N. (1965). Effects of earthquakes on dams and embankments. Geotechnique 15(2), 139-160.

Núñez. E. (2007). Uncertainties and approximations in geotechnics. Proc. XIII PCSMGE, Margarita (Venezuela), 26-39.

Seed. H. (1979). Considerations in the earthquake-resistant design of earth and rockfill dams. Geotechnique 29(3), 215-283.

Sherard. J., and Cooke. J. (1987). Concrete-face rockfill dam: I. Assessment. ASCE JGE, 113(10), 1096-1112.

Wieland. M., and Brenner. P. (2007). The Seismic performances of the concrete face rockfill dams under strong ground shaking, and discuss possible problems and deficiencies. International water power & dam construction, April 18-21.

Zeghal. M., and Ghaffar A.A. (1992). Analaysis of behavior of earth dam using strong-motion earthquake records. Journal of Geotechnical Engineering, Vol. 118, No. 2, February, 1992. ©ASCE